The effect of pressure and hot vapour residence time on the fast pyrolysis of biomass: experiments and modelling

~ Supplementary Information ~

P.S. Marathe, R.J.M Westerhof, and S.R.A. Kersten*

Sustainable Process Technology (SPT), Department of Science and Technology (TNW), University of Twente, 7522 NB, Enschede, The Netherlands

E-mail: s.r.a.kersten@utwente.nl

Phone: +31-53-489 4430. Fax: +31-53-489 4738

Experimental data

Each data point reported in Table 1 to Table 4 is an average of minimum three experiments. The calculated standard deviation on the mean is also presented. The data reported in Table 3 and Table 5, for acid-leached pinewood in fluidised bed, is based on a single experiment because of the limited availability of the feedstock.

Bagasse

Note, our results (Table 1 and 2) are inline with the data of Amutio et al.[1] who showed that the pressure has little effect on the yields of the lumped products liquid (oil), char and gas when comparing 25 kPa and 100 kPa runs. In Table 1 and 2, the reported water insoluble yield (WIS) was determined by the method described by in the literature.[2]

Table 1: Yields of oil, char, gas, water-insoluble compounds (WIS) obtained from pyrolysis of acid-leached bagasse as a function of pressure in screen-heater (T_{FS} = 515 ± 15 °C)

Pressure kPa	$\mathbf{Y_{Oil}}$	$\mathbf{Y_{Char}}$ wt.% on d.a.f. bagasse	$\mathbf{Y_{Gas}}$	$\mathbf{Y_{WIS}}$
0.005 ± 0.00	91.3 ± 1.2	4.6 ± 0.2	0.5 ± 0.0	17.2 ± 1.6
0.2 ± 0.03	85.6 ± 2.0	5.0 ± 0.4	0.5 ± 0.1	15.6 ± 2.3
2 ± 0.03	87.9 ± 0.5	3.5 ± 0.1	3.2 ± 0.6	22.1 ± 0.5
10 ± 2.5	91 ± 3	3 ± 0	3 ± 0	14 ± 0.2
21 ± 1.08	78.7 ± 2.3	9.3 ± 1.4	1.9 ± 0.4	11.8 ± 2.2
38 ± 0.30	78.5 ± 2.7	9.0 ± 1.6	2.5 ± 0.8	17.7 ± 1.3
60 ± 0.10	81.5 ± 2.9	8.7 ± 1.5	2.3 ± 0.3	18.2 ± 1.3
81 ± 1.01	79.4 ± 1.4	7.4 ± 0.5	2.9 ± 0.8	17.6 ± 1.2
101 ± 1.39	72.8 ± 2.4	8.2 ± 0.9	4.7 ± 0.3	13.3 ± 2.9

Table 2: Yield of C_6 anhydrosugars (C_6aS) and DP_1 mass fraction obtained from pyrolysis of acid-leached bagasse as a function of pressure in screen-heater (T_{FS} = 515 ± 15 °C)

Feedstock		**Untreated bagasse**				**Acid-leached bagasse**			
Pressure	±	Y_{C_6aS}	±	f_{DP_1}	±	Y_{C_6aS}	±	f_{DP_1}	±
kPa		wt.% on C_6 sugars		-		wt.% on C_6 sugars		-	
$5x10^{-3}$	0.00	25.2	0.2	0.08	0.0	73	3	0.13	0.01
0.2	0.03	16.4	1.3	0.06	0.3	67	2	0.14	0.00
2	0.03	22.0	2.9	0.05	0.3	62	2	0.18	0.00
10	2.5	-	-	-	-	51	3	0.27	0.01
20	1.08	10.2	0.9	0.10	0.3	42	2	0.32	0.00
40	0.30	10.3	1.3	0.11	0.5	42	1	0.35	0.01
60	0.10	6.8	2.2	0.15	0.1	38	1	0.42	0.00
80	1.01	8.5	1.2	0.14	0.1	38	2	0.43	0.01
100	1.39	8.1	0.8	0.15	0.0	35	1	0.39	0.00

DP distribution of C_6aS in bagasse derived pyrolysis oil

The DP distribution of C_6aS obtained from pyrolysis of bagasse is presented in Figure 1 to 5. It can be seen that for untreated-bagasse the yields of DP_1 and DP_2 are nearly independent of pressure, whereas the yields of bigger C_6aS (DP_3 to $DP_{>5}$) appear to increase slightly with a decrease in pressure. For acid-leached bagasse the yields of C_6aS as a function of pressure are much more clear and pronounced.

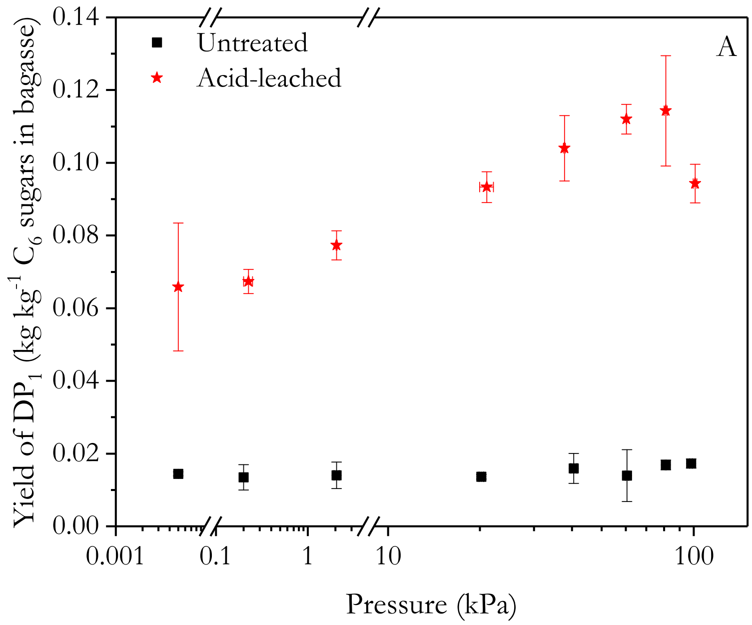

Figure 1: DP_1 yield obtained from untreated and acid-leached bagasse as a function of pressure at T_{FS} of 515 °C

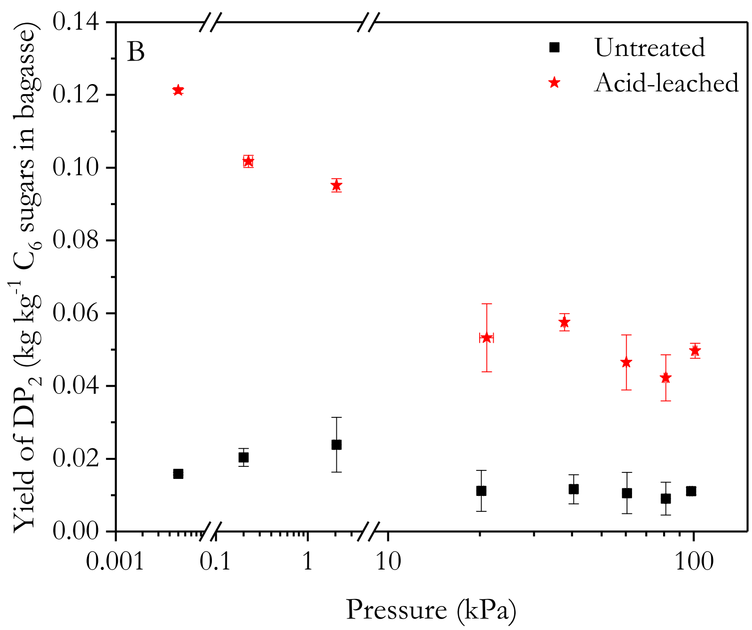

Figure 2: DP_2 yield obtained from untreated and acid-leached bagasse as a function of pressure at T_{FS} of 515 °C

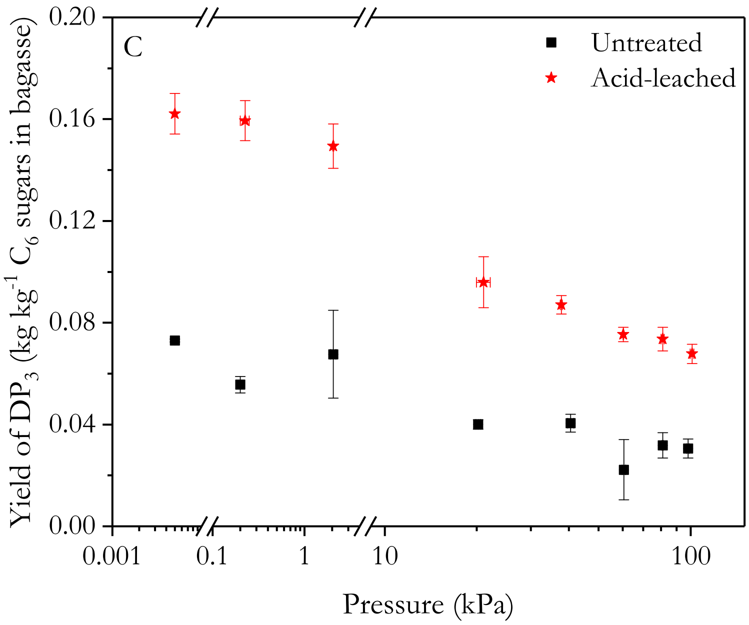

Figure 3: DP_3 yield obtained from untreated and acid-leached bagasse as a function of pressure at T_{FS} of 515 °C

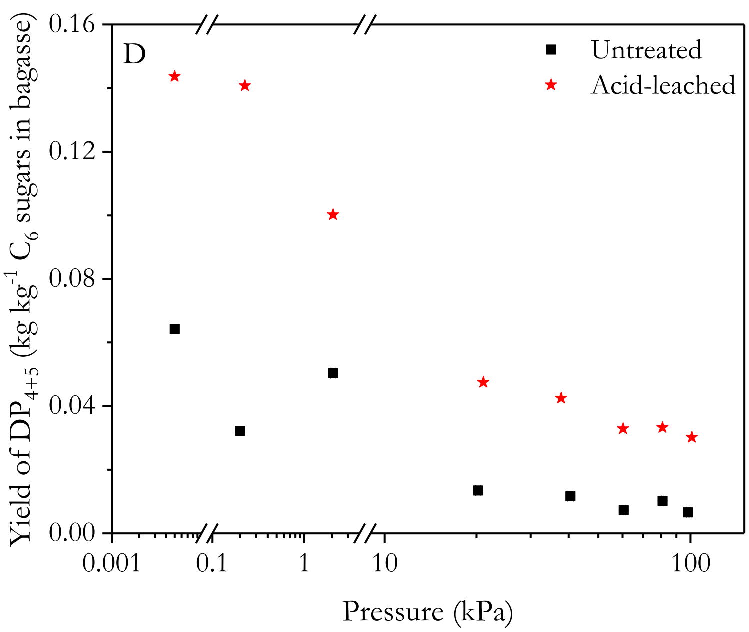

Figure 4: DP_{4+5} yield obtained from untreated and acid-leached bagasse as a function of pressure at T_{FS} of 515 °C

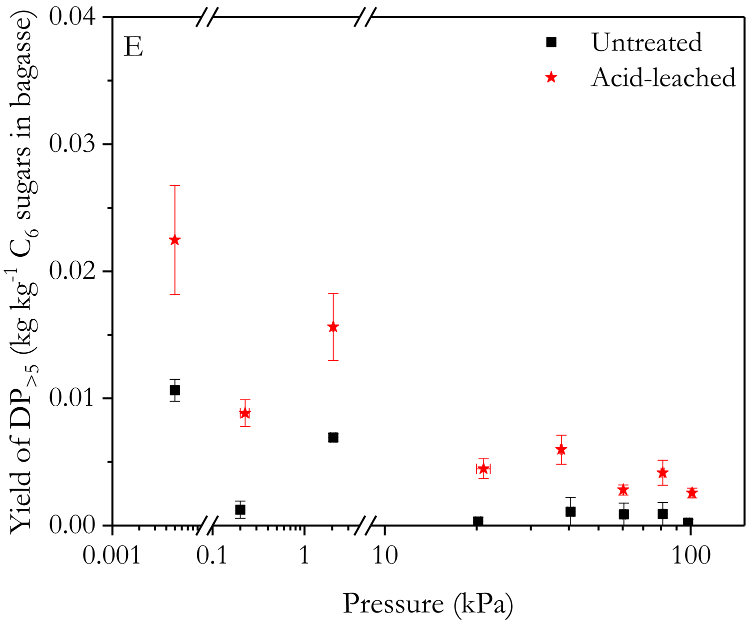

Figure 5: $DP_{>5}$ yield obtained from untreated and acid-leached bagasse as a function of pressure at T_{FS} of 515 °C

Pinewood

Table 3: Yields of oil, char, gas and water-insoluble compounds (WIS) obtained from pyrolysis of acid-leached pinewood as a function of pressure in screen-heater and fluidised bed (T = 485 °C)

Pressure	$\mathbf{Y_{Oil}}$	$\mathbf{Y_{Char}}$	$\mathbf{Y_{Gas}}$	$\mathbf{Y_{WIS}}$
kPa	wt.% on d.a.f. pinewood			
Screen-heater				
0.3 ± 0.01	83.7 ± 1.4	7.1 ± 2.2	0.5 ± 0.0	10.2 ± 0.8
50 ± 0.05	76.2 ± 1.3	8.9 ± 0.0	1.5 ± 0.2	12.7 ± 0.9
100 ± 1.3	63.6 ± 2.0	8.2 ± 0.1	2.1 ± 0.1	9.0 ± 1.0
Fluidised bed				
50	62	12	19	7.9

Table 4: Yield of C_6aS and DP_1 mass fraction obtained from pyrolysis of acid-leached pinewood as a function of pressure in screen-heater (T_{FS} = 485 ± 15 °C)

Feedstock		**Untreated pinewood**			**Acid-leached pinewood**		
Pressure		0.5 kPa	50 kPa	100 kPa	0.5 kPa	50 kPa	100 kPa
Y_{C_6aS}	kg kg^{-1} on C_6 sugars	0.22 ± 0.01	0.18 ± 0.02	0.18 ± 0.00	0.47 ± 0.03	0.40 ± 0.01	0.31 ± 0.00
f_{DP_1}	-	0.06 ± 0.01	0.16 ± 0.03	0.28 ± 0.02	0.11 ± 0.02	0.28 ± 0.01	0.44 ± 0.01

Table 5: The yield of C_6aS obtained from the pyrolysis acid-leached pinewood at 485°C and 50 kPa

DP of C_6aS	**Yield (kg kg^{-1} on C_6 sugars in on d.a.f. pinewood)**	
-	Screen-heater	Fluidised bed
1	0.11	0.26
2	0.17	0.11
3	0.08	0.01
4	0.03	0.00
5	0.00	0.00
6	0.00	0.00
Total	0.4	0.38

Direct infusion mass spectrometry

In this section, direct infusion mass spectrometry of water-soluble fraction of bio-oils and fingerprinting (MS^2) of C_6aS is presented. The details of the method are as follows. The pyrolysis oils (water-soluble fraction) were diluted with deionised water to a concentration of ~150 mg kg^{-1}. Ammonium acetate was added to the diluted oil-water mixture as an ionisation agent.[3,4] A 1 mL Hamilton syringe loaded onto a syringe pump was used to infuse diluted samples directly into the ESI chamber at a rate of 0.01 mL min^{-1}. The instrument used was an ESI Ion-Trap mass spectrometer (Bruker amaZon SL, Germany). The ESI MS analysis was accomplished in manual mode using drying temperature of 200 ℃, N_2 flowrate and nebulizer pressure of 6 L min^{-1} and 10 psi, respectively. Full scan mass spectra were acquired over the m/z range of 50 - 2000. For MS^2 experiments, helium gas was used as a collision gas with a fragmentation amplitude voltage of 1 V and a mass window was 1.5 Da.

Table 6 presents the molar mass (m/z) and NH^{4+} (or Na^+) adduct molar mass corresponding to different DPs, which were found in the oil. Different DPs found in the spectra are highlighted in a red ellipse, see Figure 6 to Figure 8.

Table 6: Molar mass (m/z) and NH^{4+} (or Na^+) adduct molar mass corresponding to different DPs

DP	**Name**	**Molar mass or m/z**	**DP with NH^{4+}**	**DP with Na^+**
-	-	Da	Da	Da
1	Levoglucosan	162	180	185
2	Cellobiosan	324	342	
3	Cellotriosan	486	504	
4	Cellotetrasan	648	666	
5	Cellopentasan	810	828	
6	Cellohexasan	972	990	

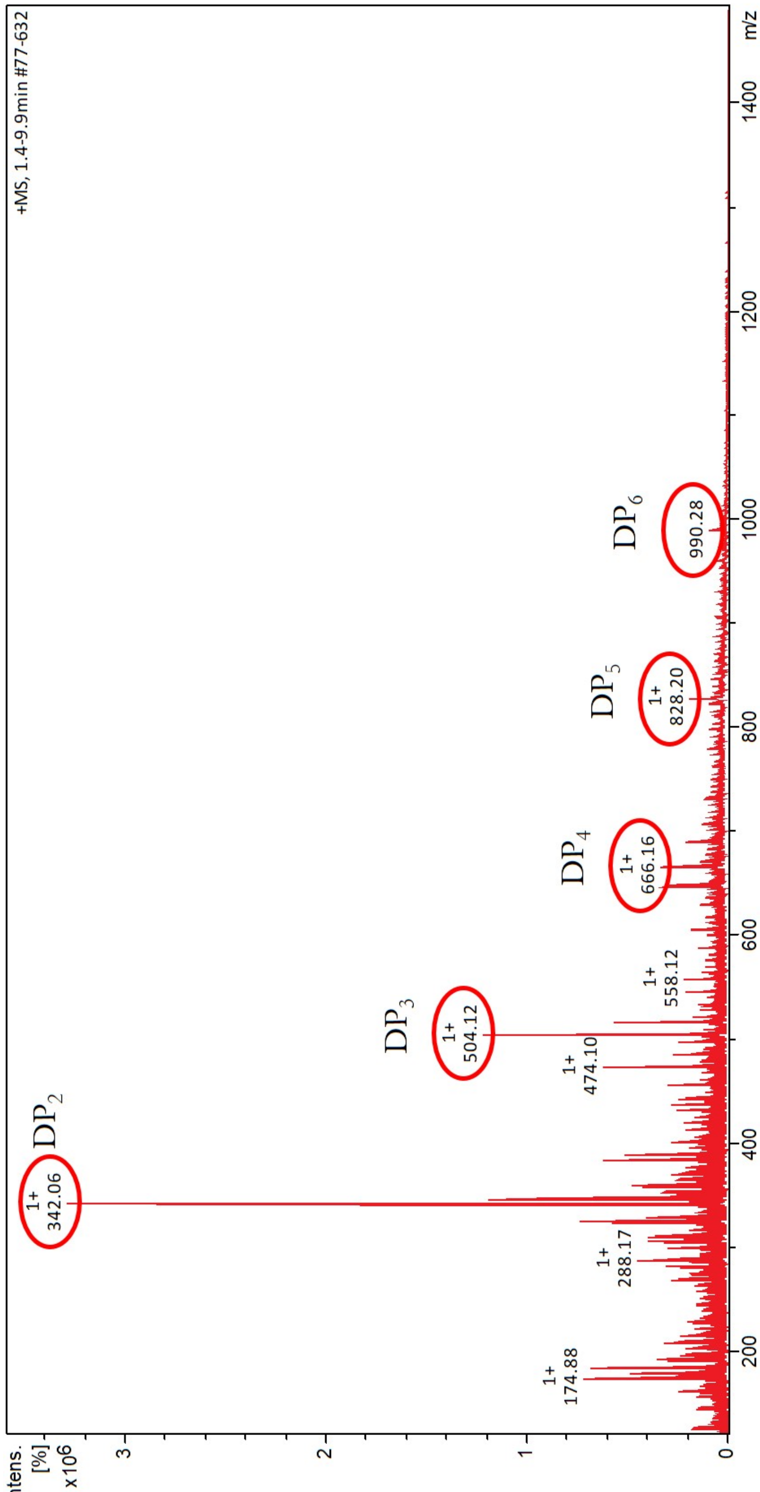

Figure 6: Mass spectrum of oil (water-soluble fraction), in a positive ion, obtained from acid-leached bagasse in a screen-heater at 0.005 kPa; TFS = 515°C

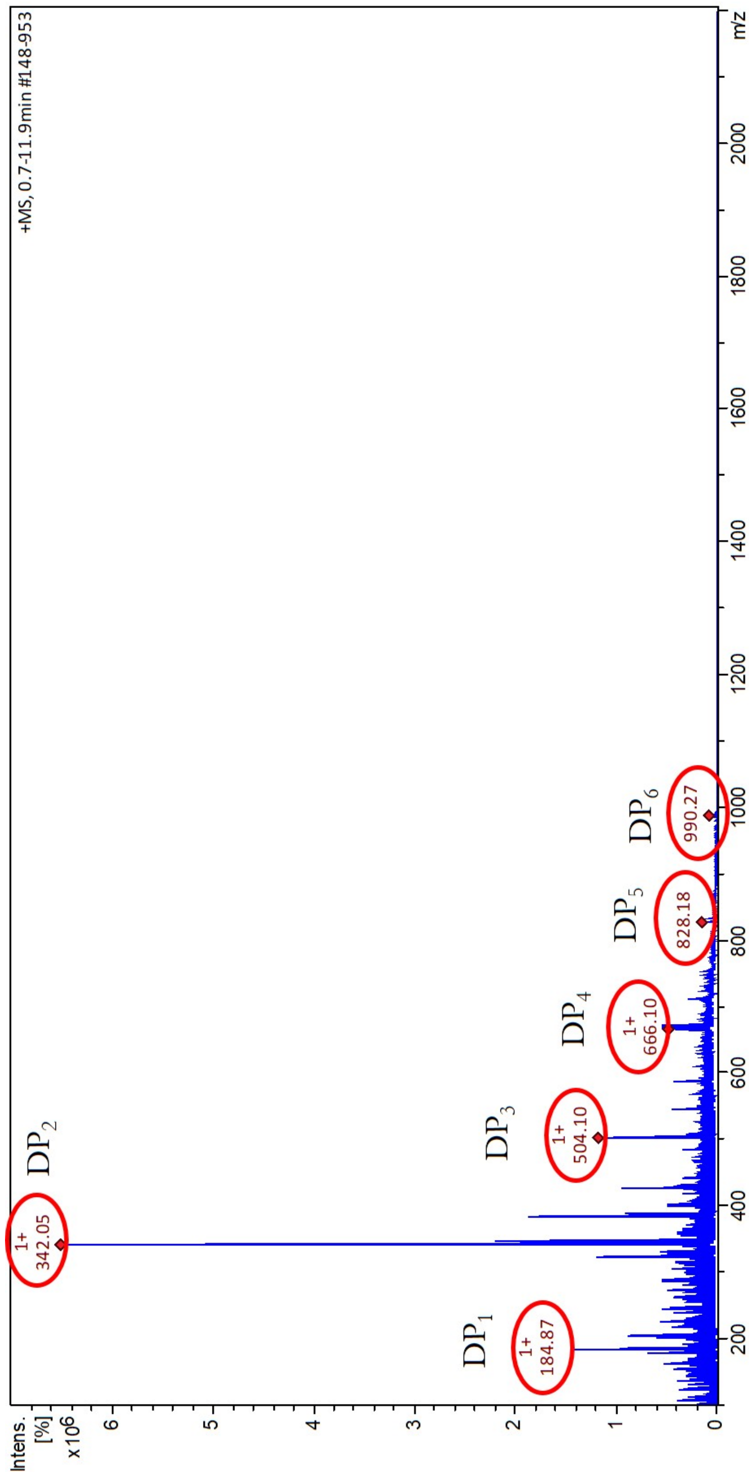

Figure 7: Mass spectrum of oil (water-soluble fraction), in a positive ion, obtained from acid-leached pinewood in a screen-heater at 50 kPa; TFS = 485°C

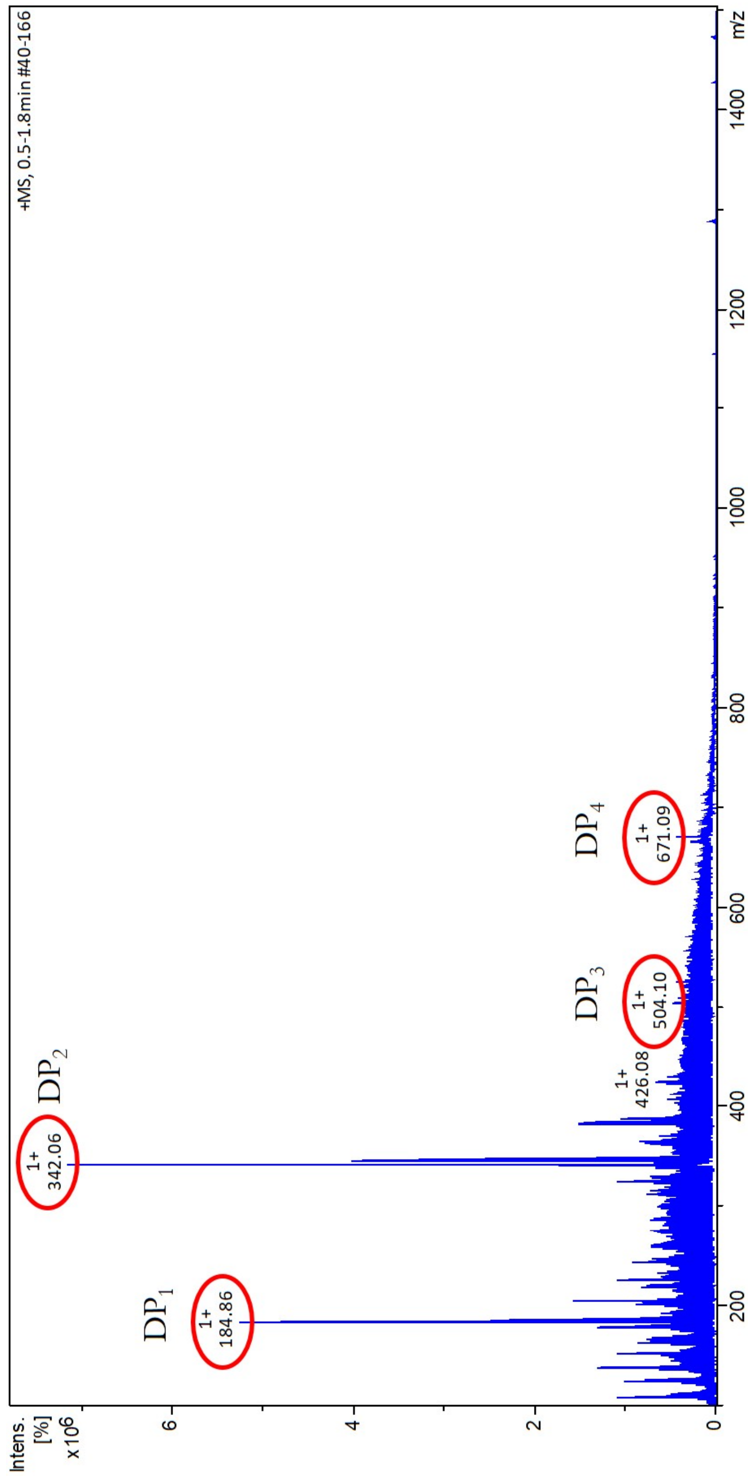

Figure 8: Mass spectrum of oil (water-soluble fraction), in a positive ion, obtained from acid-leached pinewood in a fluidised bed at 50 kPa and 485°C

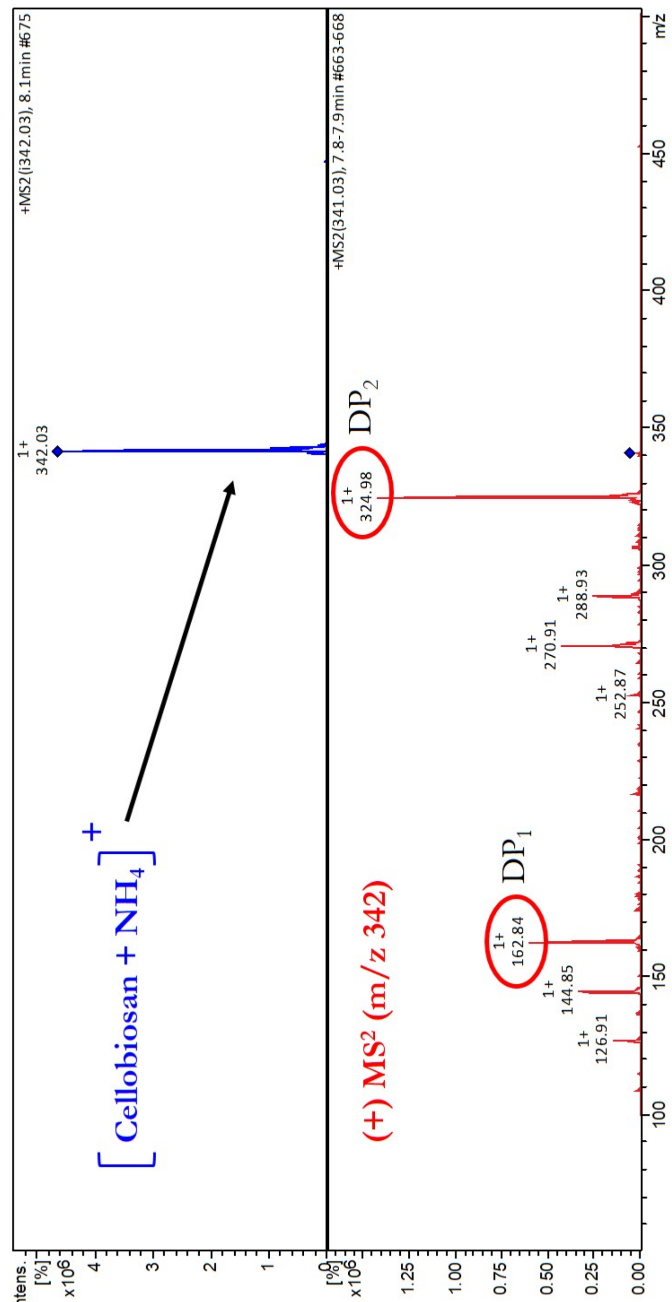

Figure 9: Product spectra from MS^2 experiments for DP_2 in a positive ion

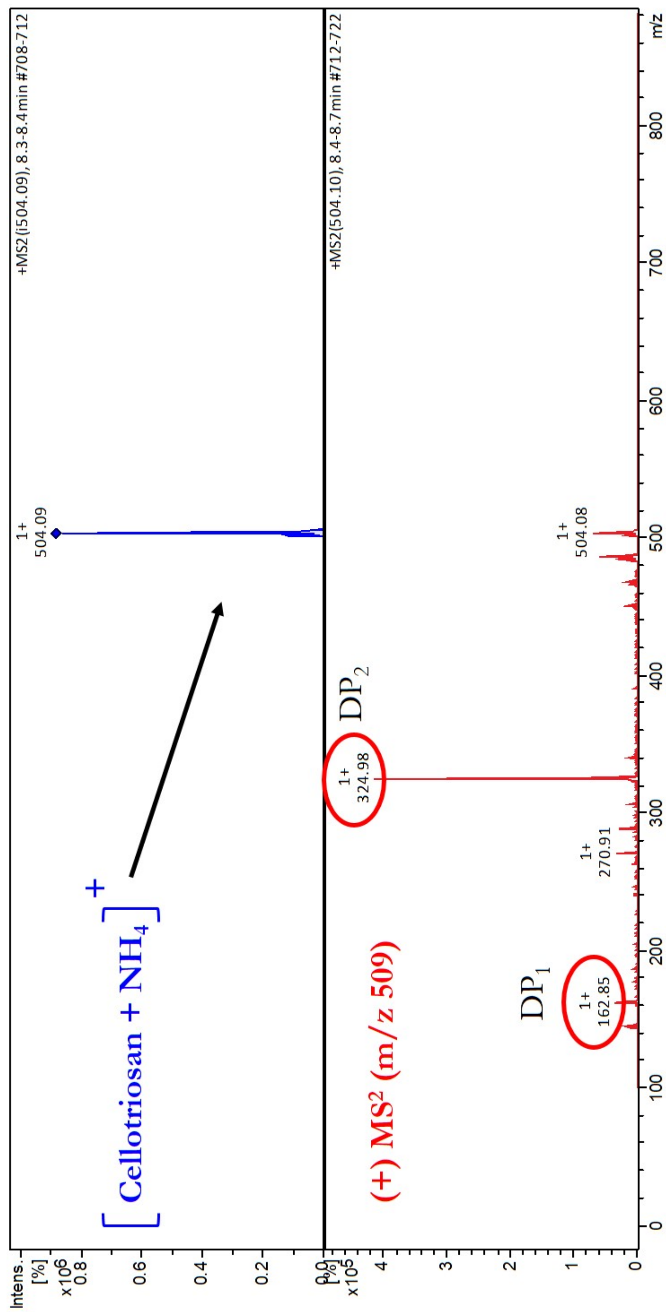

Figure 10: Product spectra from MS^2 experiments for DP_3 in a positive ion

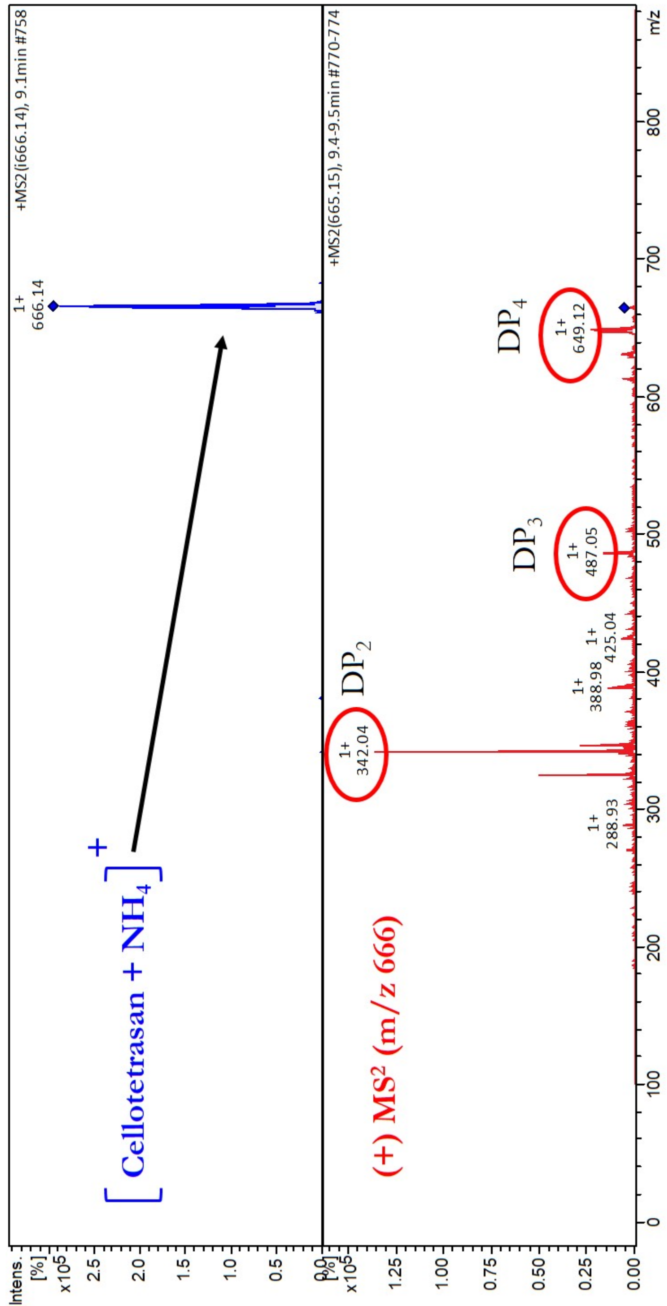

Figure 11: Product spectra from MS^2 experiments for DP_4 in a positive ion

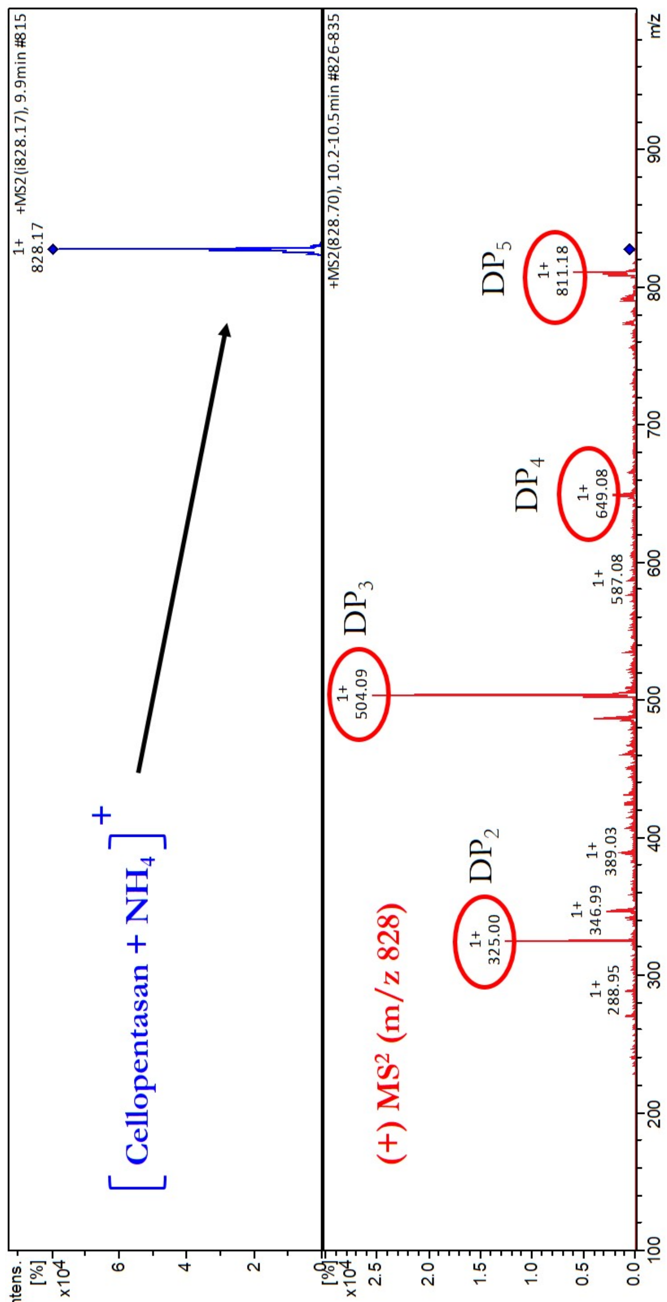

Figure 12: Product spectra from MS^2 experiments for DP_5 in a positive ion

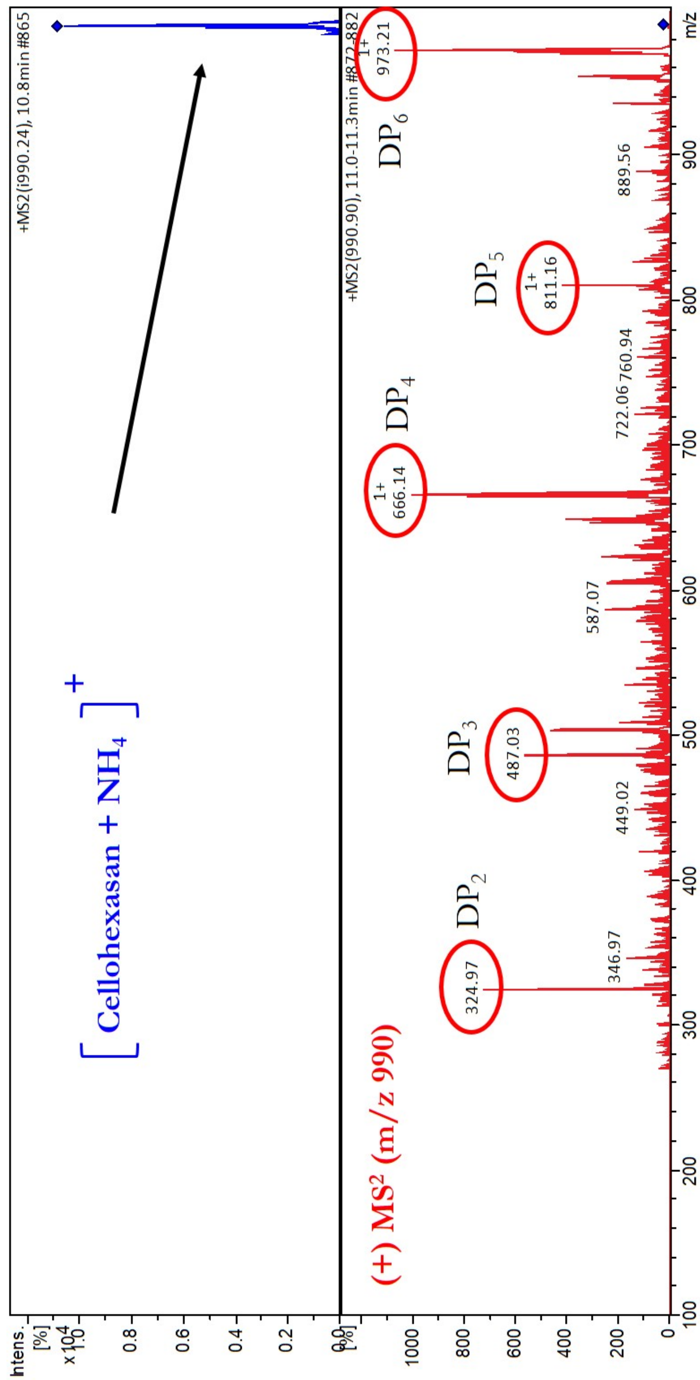

Figure 13: Product spectra from MS^2 experiments for DP_6 in a positive ion

Analytical Solution: DP_3 to DP_1 system

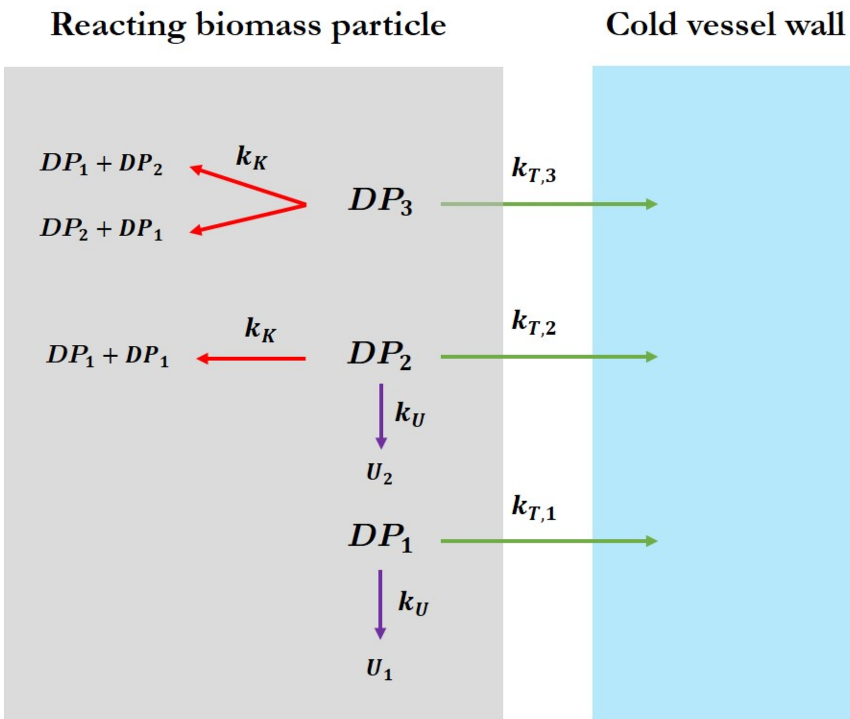

Figure 14: Schematic representation of C_6 sugars (in biomass) pyrolysis

Figure 14 shows the schematic representation of DP_3 to DP_1 system. The normalised mass balance equations for DP_3 to DP_1 in/on the particle and oil, and for U are presented below.

$$\frac{dm_{DP_3}^P}{dt} = -2k_K \; m_{DP_3}^P \tag{1}$$

$$\frac{dm_{DP_2}^P}{dt} = -(k_K + k_U + k_{T,2}) \; m_{DP_2}^P + \frac{4}{3} \; k_K \; m_{DP_3}^P \tag{2}$$

$$\frac{dm_{DP_1}^P}{dt} = -(k_U + k_{T,1}) \; m_{DP_1}^P + \frac{2}{2} \; k_K \; m_{DP_2}^P + \frac{2}{3} \; k_K \; m_{DP_3}^P \tag{3}$$

$$\frac{dm^{OS}_{DP_2}}{dt} = k_{T,2}\ m^{P}_{DP_2} \tag{4}$$

$$\frac{dm^{OS}_{DP_1}}{dt} = k_{T,1}\ m^{P}_{DP_1} \tag{5}$$

$$\frac{dm_U}{dt} = k_U\ (m^{P}_{DP_1} + m^{P}_{DP_2}) \tag{6}$$

The initial conditions are - 1) $m^{P}_{DP_3,\ t=0} = 1$, 2) $m^{P}_{DP_2,\ t=0} = m^{P}_{DP_1,\ t=0} = 0$, 3) $m^{OS}_{DP_2,\ t=0} = m^{OS}_{DP_1,\ t=0} = 0$, and 4) $m_U = 0$. Above system of ordinary differential equations (Eq. 1 to 6) is rearranged into the following matrix form,

$$\overrightarrow{x'} = A\ \overrightarrow{x} \tag{7}$$

$$\begin{bmatrix} \frac{dm^{P}_{DP_1}}{dt} \\ \frac{dm^{P}_{DP_2}}{dt} \\ \frac{dm^{P}_{DP_3}}{dt} \\ \frac{dm^{OS}_{DP_1}}{dt} \\ \frac{dm^{OS}_{DP_2}}{dt} \\ \frac{dm_U}{dt} \end{bmatrix} = \begin{bmatrix} -(k_U + k_{T,1}) & \frac{2}{2}\ k_K & \frac{2}{3}\ k_K & 0 & 0 & 0 \\ 0 & -(k_K + k_U + k_{T,2}) & \frac{4}{3}\ k_K & 0 & 0 & 0 \\ 0 & 0 & -2\ k_K & 0 & 0 & 0 \\ k_{T,1} & 0 & 0 & 0 & 0 & 0 \\ 0 & k_{T,2} & 0 & 0 & 0 & 0 \\ k_U & k_U & 0 & 0 & 0 & 0 \end{bmatrix} \times \begin{bmatrix} m^{P}_{DP_1} \\ m^{P}_{DP_2} \\ m^{P}_{DP_3} \\ m^{OS}_{DP_1} \\ m^{OS}_{DP_2} \\ m_U \end{bmatrix} \tag{8}$$

Note, inbuilt symbolic toolbox of Matlab®2017a was used to obtain the eigenvalues (λ) and eigenvectors ($\overrightarrow{\eta}$) of Eq. 8. The general solution of the system of ordinary differential equations is given by Eq. 9

$$\overrightarrow{x_i}(t) = \sum_{i=1}^{6} c_i \; e^{\lambda_i t} \overrightarrow{\eta_i} \tag{9}$$

At $t \rightarrow \infty$

$$m^{P}_{DP_1} = m^{P}_{DP_2} = m^{P}_{DP_3} = 0 \tag{10}$$

$$m^{OS}_{DP_1} = \frac{k_{T,1}(3k_K + k_{T,2} + k_U)}{3(k_{T,1} + k_U)(k_K + k_{T,2} + k_U)} \tag{11}$$

$$m^{OS}_{DP_2} = \frac{2k_{T,2}}{(3k_K + k_{T,2} + k_U)} \tag{12}$$

$$m_U = \frac{k_U(3k_K + 2k_{T,1} + k_{T,2} + 3k_U)}{3(k_{T,1} + k_U)(k_K + k_{T,2} + k_U)} \tag{13}$$

Eq. 14 and Eq. 15 calculate the yield of C_6aS and the mass fraction of DP_1 in C_6aS, respectively.

$$\begin{aligned} Y_{C_6as} &= 1 - Y_U \\ &= 1 - \frac{m_{U,t=\infty}}{m^{P}_{DP_3,t=0}} \\ &= \frac{k_U(k_K + k_U + \frac{2}{3}k_{T,1} + k_{T,2})}{(k_{T,1} + k_U)(k_K + k_{T,2} + k_U)} \end{aligned} \tag{14}$$

$$\begin{aligned} f_{DP_1} &= \frac{m^{OS}_{DP_1,t=\infty}}{m^{OS}_{DP_1,t=\infty} + m^{OS}_{DP_2,t=\infty}} \\ &= \frac{3k_K k_{T,1} + k_{T,1}k_{T,2} + k_{T,1}k_U}{3k_K k_{T,1} + 3k_{T,1} + k_{T,2} + k_{T,1}k_U + 2k_{T,2}k_U} \end{aligned} \tag{15}$$

Model results

Total fit procedure

The C_6aS yield (on C_6 sugars in acid-leached bagasse) and the mass fraction of DP_1 in C_6aS predicted using the total fit procedure are presented in Figure 15.

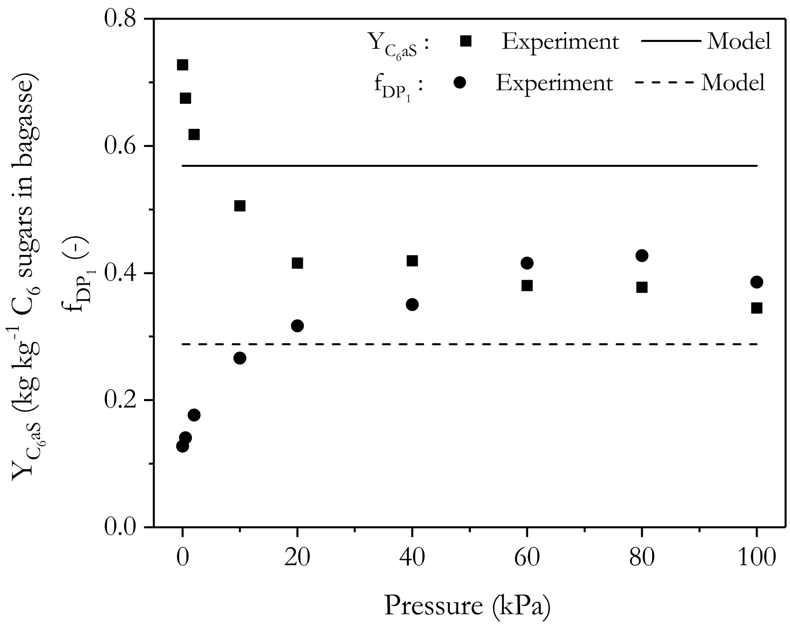

Figure 15: C_6aS yield (on C_6 sugars in acid-leached bagasse) and the mass fraction of DP_1 in C_6aS, experimental and calculated using the total fit procedure, as a function of pressure

Individual fit procedure

Parity plot of the experimental C_6aS yield (on C_6 sugars in acid-leached bagasse) and the mass fraction of DP_1 against their predicted values using individual fit procedure are presented in Figure 16. The values of $\frac{k_{T,avg}}{k_K+k_U}$ per pressure obtained using the individual fit procedure are presented in Table 7.

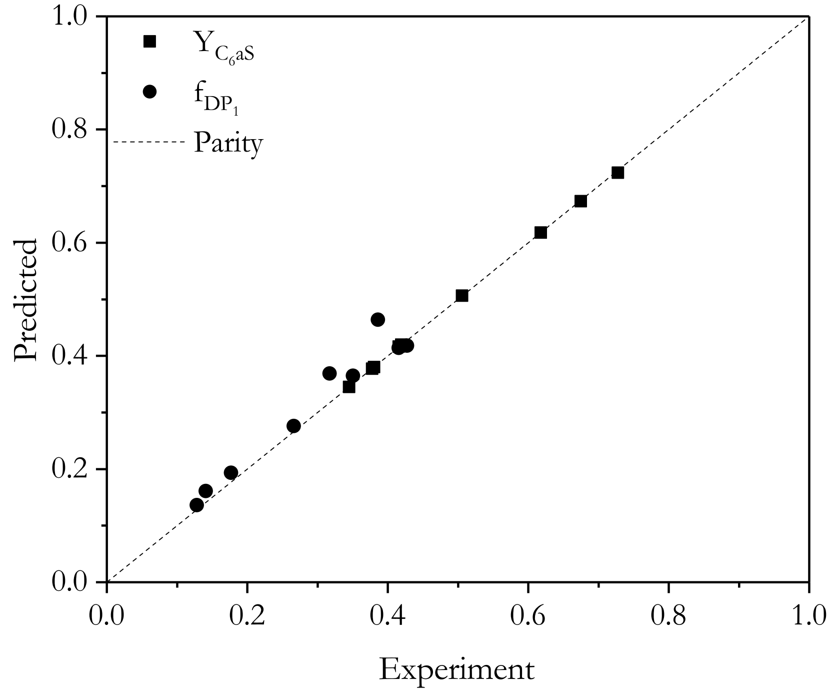

Figure 16: Parity plot in which the experimental C_6aS yield (on C_6 sugars in acid-leached bagasse) and the mass fraction of DP_1 are plotted against their predicted values using individual fit procedure

Table 7: Values of $\frac{k_{T,avg}}{k_K+k_U}$ per pressure obtained using the individual fit procedure

Pressure kPa	$\frac{k_{T,avg}}{k_K+k_U}$ -
0.005	1.9 ± 0.9
0.5	1.5 ± 0.5
2	1.2 ± 0.3
10	0.8 ± 0.2
20	0.5 ± 0.2
40	0.5 ± 0.1
60	0.4 ± 0.1
80	0.4 ± 0.1
100	0.4 ± 0.1

Correlation between $\frac{k_{T,avg}}{k_K+k_U}$ and pressure

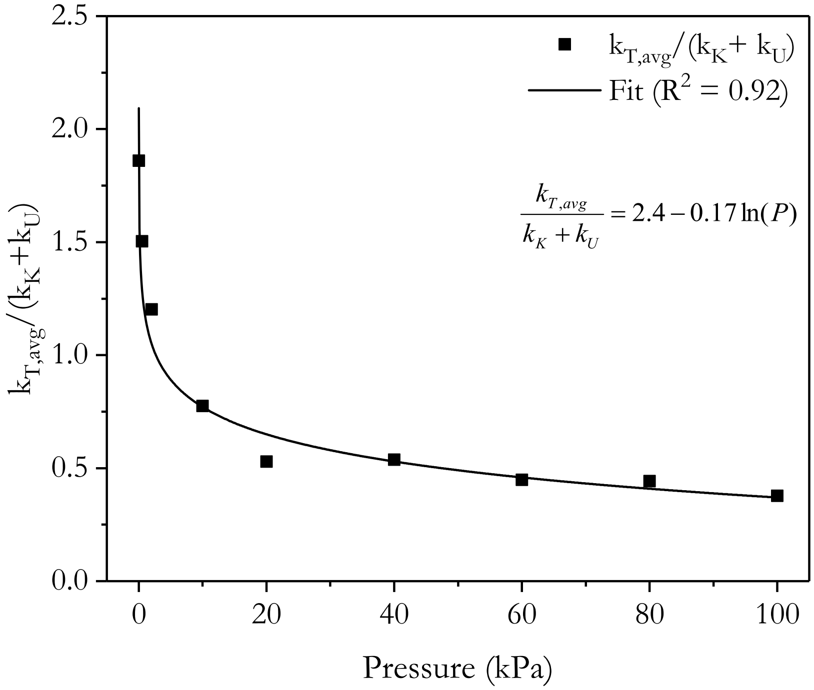

Figure 17: Values of $\frac{k_{T,avg}}{k_K+k_U}$ obtained using individual fit procedure as a function of the pressure with fixed $\frac{k_K}{k_K+k_U}$ obtained from total fit procedure

References

(1) Amutio, M.; Lopez, G.; Aguado, R.; Artetxe, M.; Bilbao, J.; Olazar, M. Effect of Vacuum on Lignocellulosic Biomass Flash Pyrolysis in a Conical Spouted Bed Reactor. *Energy & Fuels* **2011**, *25*, 3950–3960.

(2) Scholze, B.; Meier, D. Characterization of the water-insoluble fraction from pyrolysis oil (pyrolytic lignin). part i. PY–GC/MS, FTIR, and functional groups. *Journal of Analytical and Applied Pyrolysis* **2001**, *60*, 41–54.

(3) Alsbou, E.; Helleur, B. Direct Infusion Mass Spectrometric Analysis of Bio-oil Using ESI-Ion-Trap MS. *Energy & Fuels* **2013**, *28*, 578–590.

(4) Westerhof, R. J. M.; Oudenhoven, S. R. G.; Marathe, P. S.; Engelen, M.; Garcia-Perez, M.; Wang, Z.; Kersten, S. R. A. The interplay between chemistry and heat/mass transfer during the fast pyrolysis of cellulose. *Reaction Chemistry & Engineering* **2016**, *1*, 555–566.